CRYSTAL GROWTH & DESIGN
2009
VOL. 9, NO. 3
1378–1384

# The Impact of Direct Nucleation Control on Crystal Size Distribution in Pharmaceutical Crystallization Processes

Mohd R. Abu Bakar, Zoltan K. Nagy,* Ali N. Saleemi, and Chris D. Rielly

*Department of Chemical Engineering, Loughborough University, Loughborough, Leicestershire, LE11 3TU, United Kingdom*

*Received June 9, 2008; Revised Manuscript Received December 5, 2008*

**ABSTRACT:** The control of crystal size distribution (CSD) in pharmaceutical crystallization is of primary importance, as downstream processes such as filtration or drying are greatly affected by the properties of the CSD. It is recognized that the variability in the final CSD is mainly caused by the significant uncertainties in the nucleation rates, and therefore, a good control of nucleation events is necessary to achieve the desired CSD. In this paper, a new direct nucleation control (DNC) approach is introduced that directly controls the apparent onset of nucleation defined as the formation of new particles with detectable size using *in situ* instruments. The approach uses information on nucleation and dissolution, provided by focused beam reflectance measurement (FBRM), in a feedback control strategy that adapts the process variables, so that the desired quality of product is achieved, for example large crystals with a narrow CSD. In addition, DNC provides *in situ* fines removal through the operating protocol, rather than having additional equipment and external recycle loops. DNC does not require concentration measurement and has the advantage of being a model-free approach, requiring no information on nucleation or growth kinetics in order to design an operating curve. The DNC approach automatically and adaptively detects the boundary of the operating zone; hence it is more robust to the presence of impurities or residual solvent than the supersaturation control approach. The approach has been applied for the crystallization of glycine and experimental results demonstrate the benefits of DNC of producing larger crystals with narrower CSD compared to classical operations.



## 1. Introduction

Crystallization is an important unit operation used in a variety of industries. It is estimated that more than 80% of pharmaceutical products involve at least one crystallization step in their manufacturing process.[1] The crystallization operation is often critical because it determines product properties such as the crystal size distribution (CSD), habit and polymorphic form. The CSD is of primary importance since it influences subsequent downstream operations such as filtration and drying, and the product performance such as dissolution and bioavailability. Along with the United States Food and Drug Administration's (FDA) Process Analytical Technology (PAT) initiative, the development of control approaches, which can improve the manufacturing of products with desired properties, has become of significant interest.[2−4]

The majority of control approaches applied in crystallization affect the CSD indirectly by implementing a temperature or antisolvent profile in time to follow a given supersaturation profile in the phase diagram.[5,6] These profiles are obtained either using simple trial-and-error experimentation or more complex model-based[6,7] or direct-design approaches.[8−13] However, it is recognized that the variability in the final CSD is mainly caused by the significant uncertainties in the nucleation rate, and all of the above-mentioned approaches in essence try to identify operating protocols, which provide an acceptable compromise between crystal growth and nucleation.[3,14]

Lasentec focused beam reflectance measurement (FBRM) is one of the *in situ* instruments that has been used extensively in the crystallization processes to provide qualitative as well as quantitative information about nucleation and crystal growth.[15−21] Although FBRM cannot give direct information about the formation of critical clusters, the evolution of the counts of the newly formed particles (after nucleation and growth to the detectable size) and the chord length distribution provide valuable information, which can be indirectly related to the nucleation, growth, agglomeration or attrition phenomena during the crystallization process.[21] Despite the widespread use of FBRM for monitoring crystallization processes, up until now only a few attempts have been reported that use online FBRM information to augment existing crystallization operations[18,22−26] with almost all cases of FBRM being used in conjunction with supersaturation control approaches. In this paper a novel approach will be introduced that directly controls the onset of nucleation in the case of (i) antisolvent and (ii) combined cooling and antisolvent crystallization processes. A desired number of FBRM counts, which indicate the number density of crystals, is maintained during the entire duration of crystallization using a feedback control strategy that adapts the antisolvent/solvent addition, or cooling/heating rate, to directly control the nucleation or dissolution rates. The experimental results from the implementation of the DNC approach for the crystallization of glycine are reported below.

## 2. Direct Nucleation Control Approach

Direct nucleation control (DNC) is a model-free approach in which the number of counts measured by the FBRM is directly controlled using a feedback control strategy. By definition, the total number of counts/s (#/s) measured by FBRM is the sum of the number of chord length measurements detected in all the channels (1 through 38 in the FBRM model used) that represents a chord length range from 0.8 to 1000 $\mu$m, and is approximately proportional to the nucleation rate, which is the predominant mechanism in changing the number of particles. Figure 1 shows the schematic block diagram of the DNC approach for antisolvent crystallization systems. A similar structure can be used for cooling crystallization.

A typical operating profile during DNC, represented in the phase diagram, is illustrated in Figure 2. The DNC approach automatically switches between heating and cooling, or solvent

* Corresponding author. Phone: + 44 (0)1509 222 516. Fax: + 44 (0)1509 223 953. E-mail: Z.K.Nagy@lboro.ac.uk.

10.1021/cg800595v CCC: $40.75 
Published on Web 01/15/2009

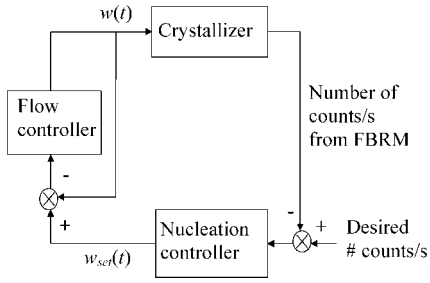


**Figure 1.** A block diagram of the DNC approach. $w(t)$ is the actual antisolvent/solvent flowrate into the crystallizer; $w_{set}(t)$ is the antisolvent/solvent flowrate set-point given by the DNC to the pump.

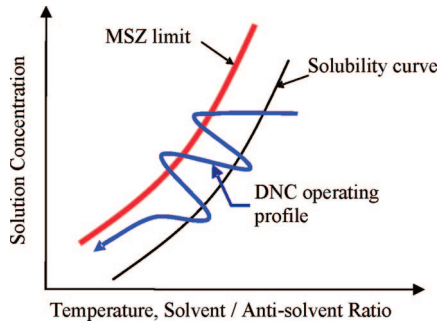


**Figure 2.** Typical DNC operating profile.

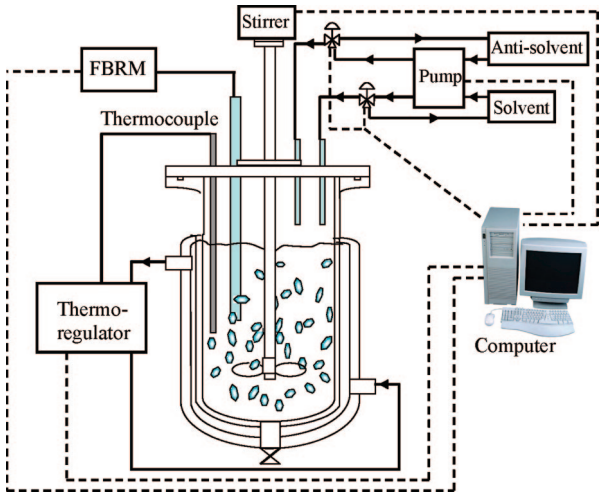


**Figure 3.** A schematic representation of the experimental setup for DNC experiments.

and antisolvent addition, or a combination of the two, to generate nucleation, or fines dissolution, to maintain the desired number of counts/s. If the number of counts/s exceeds the desired value, the excess particles are dissolved by solvent addition, or an increase in temperature, which drives the process into the undersaturated zone until the number of counts/s decreases. The proposed DNC approach provides *in situ* fines removal through the operating protocol, rather than having additional equipment and external recycle loops. The method extends the fines removal strategy proposed by Lewiner et al.[27] in which the online measurement signal is not only used for the monitoring purposes but also as an input for a continuous feedback control methodology.

An additional novel characteristic of the DNC is that it does not use predetermined heating or cooling polices. The heating/cooling rates (or solvent/antisolvent addition rates) are automatically determined during the entire duration of the crystallization in correlation with the extent of nucleation detected. The DNC approach has the benefit of automatically driving the crystallization process toward the optimal operating curve by automatically and adaptively detecting the metastable zone limits. It provides a very robust methodology for crystallization scale-up, through FBRM feedback control, which requires virtually no *a priori* information about the model, kinetics or metastable zone width of the process. Since the approach tends to operate at high supersaturation, the problems related to solvent-inclusion, impurities and agglomeration may be facilitated. Usually in these

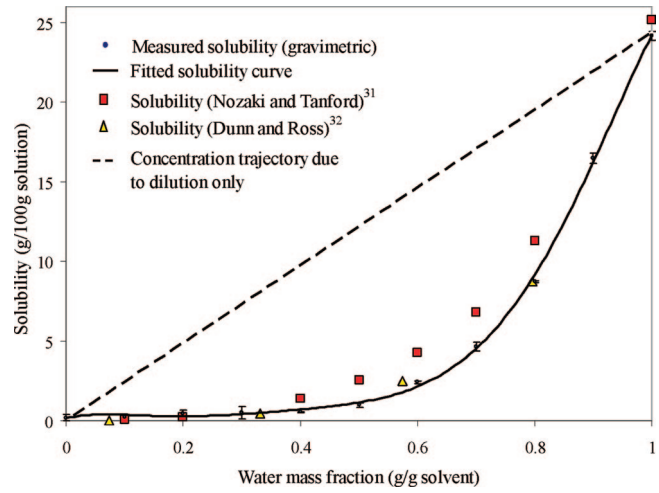


**Figure 4.** Solubility data and trajectory of the solution concentration due to the dilution as a result of the addition of antisolvent.

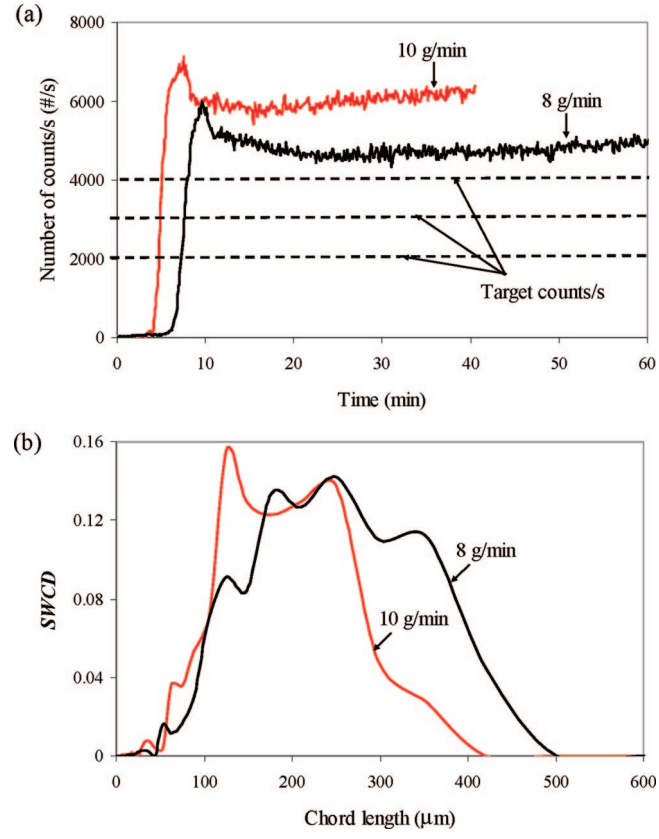


**Figure 5.** Profiles of (a) number of counts/s and (b) SWCD for the uncontrolled experiments with antisolvent addition rates of 8 g/min and 10 g/min. The dashed lines are the target counts/s.

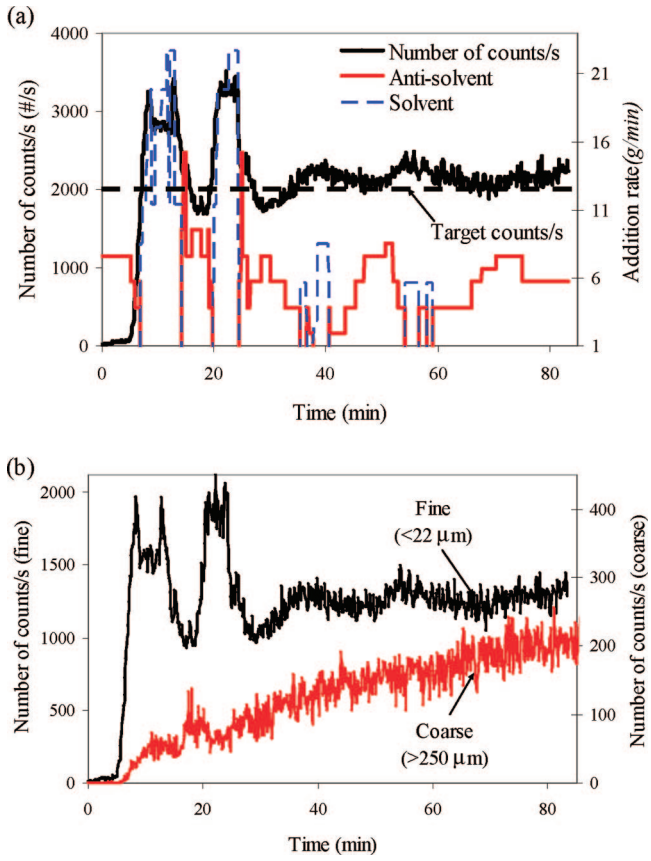


**Figure 6.** Profiles of (a) number of counts/s and antisolvent/solvent addition rate, and (b) number of fines and coarse for DNC experiment at a desired number of counts/s of 2000 #/s.

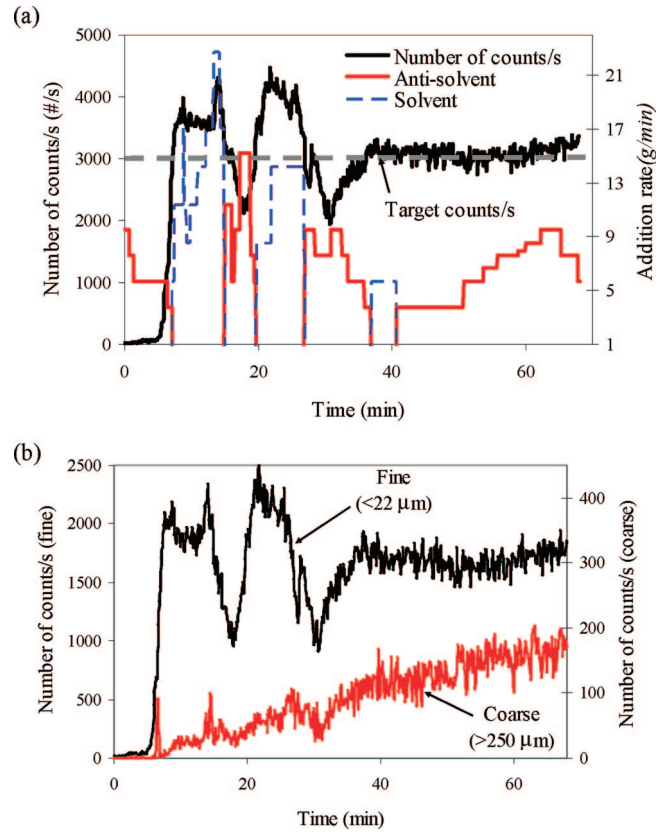


**Figure 7.** Profiles of (a) number of counts/s and antisolvent/solvent addition rate, and (b) number of fines and coarse for DNC experiment at a desired counts/s of 3000 #/s.

cases it is recommended to operate at lower supersaturation. However, the repeated and controlled dissolutions have a deagglomeration effect on the system with the potential additional benefit of minimizing solvent or impurity inclusion due to agglomeration. The approach provides a simple and robust inferential control method of the size distribution by maintaining the number of counts/s constant, hence eliminating the difficulties related to the conversion of chord length distribution (CLD) to CSD, which would be required by more sophisticated algorithms, such as nonlinear model predictive control.[28]

The DNC approach can also be extended to control polymorphic transformations. This however requires the polymorphic system to exhibit a distinguishable shape change upon transformation, or show a separate nucleation event, which can be correlated with FBRM signal. The approach is different from the recently published robust model based approaches[29] in that it is model-free and does not require model development, parameter estimation and optimization. The DNC approach could be more favorable in an industrial environment as the iterative way of modeling and experiment may consume significantly more resources and time.

## 3. Experimental Section

**3.1. Materials.** In all experiments, aqueous glycine (>99.5% purity, Fisher BioReagents) solutions were prepared, corresponding to a solubility of 22.5 g of glycine per 100 g of water at 20 °C.[30] Glycine was dissolved in water by heating to 35 °C at a rate of 5 °C/min. After the solution equilibrated at 35 °C for 10 min, the temperature of the solution was lowered to 30 °C with a cooling rate of 1 °C/min, after which the temperature was further reduced to 25 °C at 0.3 °C/min. The temperature of the solution was maintained at 25 °C prior to the start of experiment. Ethanol (99.99% purity, analytical reagent grade, Fisher Scientific) was used as an antisolvent.

**3.2. Apparatus.** The crystallization experiments were performed in a jacketed 1000 mL glass vessel. The temperature in the vessel was controlled with a stainless steel Pt100 thermocouple connected to a thermofluid (Dow Corning 200/20 cS) circulator bath (Huber Ministat 125). The temperature readings were recorded every 4 s on a computer by a control interface written in LabVIEW (National Instruments). An overhead stirrer with a stainless steel three-blade marine type impeller was used to agitate the system at 400 rpm. This agitation speed was chosen to be high enough to guarantee that particles are well suspended throughout the process, but low enough to avoid attrition or generation of bubbles due to vortex formation. A FBRM probe (model A100, Lasentec) was inserted into the solution to measure chord length distributions in the range 0.8 to 1000 $\mu$m (the lower limit therefore requires nucleation plus some growth to occur before detection occurs in the FBRM). The position and orientation of the probe were chosen according the standard recommendations to avoid particles adhering to the probe and provide suitable sampling. The distributions were collected every 6 s and averaged during collection. They were monitored using the control interface software (version 5.3). The solvent and antisolvent were pumped into the vessel by a MasterFlex console driver with EasyLoad II peristaltic pump, calibrated before the experiments. Two-way solenoid valves were used for the alternate addition of solvent/antisolvent, which was controlled by the computer. A schematic representation of the experimental setup is shown in Figure 3.

**3.3. Solubility of Glycine in Water−Ethanol Mixture.** The method to determine the solubility of glycine in a mixture of water−ethanol was based on the one that used by Nozaki and Tanford.[31] Glass tubes containing glycine in various compositions of water−ethanol mixture were shaken for 24 h in a water bath maintained at 25 °C. The solutions were separated from the solids by filtration through 0.45 $\mu$m syringe filters, while the tubes were kept partially immersed in the bath. The supernatants obtained were transferred into evaporating dishes, which were weighted before the transfer and weighted again after the transfer. The supernatants on the dishes were assayed by a gravimetric method that involves evaporation overnight in a vacuum oven, approximately

12 h at 35 °C initially, and then the temperature of the oven was increased to 107 °C. The evaporating dishes were weighted until constant weights were obtained.

**3.4. Uncontrolled Antisolvent Addition.** This experiment was conducted to see the maximum total counts/s the system could achieve, so that the value can be used as an upper limit, below which a suitable desired value of counts/s could be selected for the subsequent controlled experiments. The procedure involved the continuous addition of antisolvent to an aqueous glycine solution at two fixed rates of 8 g/min and 10 g/min until the number of counts/s stabilized.

**3.5. DNC by Antisolvent/Solvent Addition.** In this experiment, the desired number of counts/s was selected based on the maximum counts/s achieved in the uncontrolled antisolvent addition experiment described previously. Antisolvent was added to the aqueous glycine solution until primary nucleation occurred and was detected by the FBRM, after which the addition rate was reduced or stopped to avoid an overshoot from the desired number of counts/s. Once the number of counts/s exceeded the desired value, the addition of antisolvent was stopped and, sequentially, solvent was added to dissolve the fine particles, thus correcting the number of counts/s. The antisolvent was continuously added at a slow rate toward the end of the batch to ensure that the supersaturation in the system is maintained without triggering nucleation. The experiment was stopped once the suspension reached the 1000 mL mark on the vessel. The crystals produced were filtered and dried for subsequent analysis. This procedure was repeated with different desired numbers of counts/s. The solvent/antisolvent addition rate was determined according to a proportional control algorithm based on the error between the desired and measured number of counts/s. According to this approach, as the number of counts/s starts to increase, the antisolvent addition rate is decreased and switched to solvent addition as soon as the number of counts/s exceeds the desired value. Similarly, during the solvent addition, the addition rate was also in correlation with the error between the desired and measured number of counts/s. The decrease in the number of counts/s due to the dilution effect during solvent/antisolvent addition was also considered (see Figure 4).

**3.6. DNC by Combined Antisolvent Addition and Heating−Cooling.** This experiment follows the same procedure as described in section 3.4, but instead of adding solvent, heating was used to correct the nuclei count, should the generation of nuclei exceed the desired number of counts/s. Once the desired number of counts/s was achieved, the supersaturation was continuously generated through either cooling or antisolvent addition.

## 4. Results and Discussion

**4.1. Solubility of Glycine in Water−Ethanol Mixture.** Although the proposed DNC approach does not require any information about the solubility of the crystallizing system, they were determined in this work to provide useful guidelines for the method of supersaturation generation as well as acting as lower limits for the crystallization operating profiles. The solubility values obtained in this study are compared with the literature values from the work of Nozaki and Tanford,[31] and Dunn and Ross[32] as shown in Figure 4. Based on the figure, the experimental values appear to be in agreement with the results obtained by Dunn and Ross, but slightly below the results obtained by Nozaki and Tanford. A trajectory of solution concentration due to dilution as a result of the antisolvent addition, calculated based on mass balance, is also shown in the figure.

**4.2. Uncontrolled Antisolvent Addition.** Figure 5(a) shows the history of the number of counts/s measured by FBRM from the start of the antisolvent addition (at $t = 0$). Once nucleated, the number of counts/s increased very rapidly to almost 7000 #/s for the higher addition rate of antisolvent and 6000 #/s for the lower addition rate, after which they dropped slightly and eventually stabilized at 6000 #/s and 5000 #/s, respectively. This result is to be expected because the higher the supersaturation generation rate, the greater the number of nuclei that will form. The subsequent drop in counts/s may be due to a combinational effect of Ostwald ripening and dilution. Dilution is suggested because the sudden formation of nuclei produced a rapid reduction in the solute concentration and together with the continuous addition of antisolvent resulted in the dissolution of some small crystals. Based on the result of this experiment, three target numbers of counts/s for the subsequent DNC experiments were selected, i.e. 2000, 3000 and 4000 #/s, as shown in Figure 5(a).

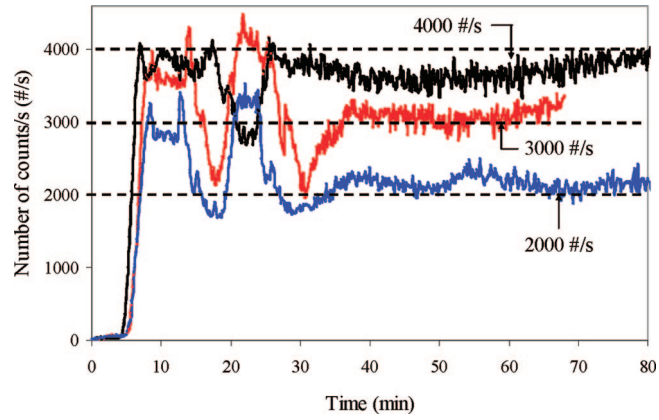


**Figure 8.** Profile of the number of counts/s for DNC experiments at 2000, 3000 and 4000 #/s.

In order to get information about the size of the crystals, the square-weighted mean chord length (SWMCL) statistic was used, defined as

$$\mathrm{SWMCL} = \frac{\sum_{i=1}^{k} n_i M_i^3}{\sum_{i=1}^{k} n_i M_i^2} \quad (1)$$

where $M_i$ is the midpoint length of an individual channel $i$, $k$ is the number of measurement channels and $n_i$ is the number of counts/s in an individual measurement channel. The SWMCL statistic was found to resemble more closely the Sauter mean diameter measured using laser diffraction instrument[33,34] and optical microscopy.[17,34] The square-weighted chord distribution (SWCD) is defined as

$$\mathrm{SWCD} = \frac{n_i M_i^2}{\sum_{i=1}^{k} n_i M_i^2} \quad (2)$$

The FBRM data do not correspond quantitatively to laser diffraction or optical microscopic data, since they are based on different principles of measurement, however the trends could be analyzed to give information about the dynamic progress of the crystallization process.

As indicated by the profile of the SWCD in Figure 5(b), due to the more intense nucleation rate for the higher antisolvent addition rate, the competition between growth and nucleation for the solute molecules increases and as a result, the size of the crystals produced is smaller.

**4.3. DNC by Antisolvent/Solvent Addition.** Figure 6(a) shows the profiles of the number of counts/s and the antisolvent/solvent addition rate for a DNC target of 2000 #/s. It can be seen from the profile that there were a couple of overshoots and undershoots before the system finally reached the desired

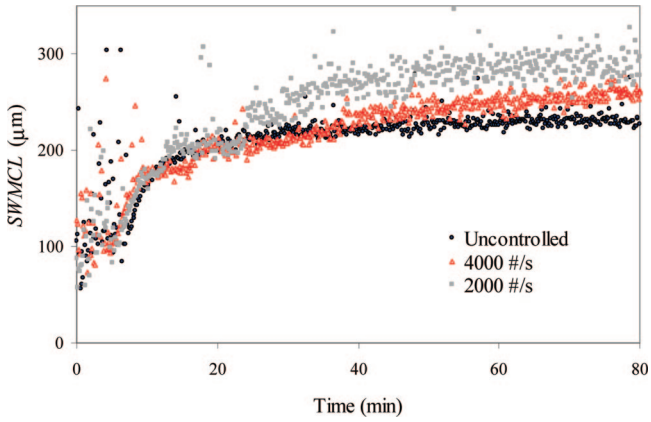


**Figure 9.** Profile of the SWMCLs for the uncontrolled and DNC experiments at 2000 and 4000 #/s.

number of counts/s. It was found that primary nucleation is always difficult to control as the increase in number of counts/s after the onset of nucleation is very fast.

Figure 6(b) shows the evolution of fine and coarse crystals during DNC. Fines were defined to be $<22\ \mu$m, whereas coarse particles were defined to be $>250\ \mu$m. The trend shows that solvent addition decreases the amount of fines, while having little effect on the number of coarse crystals. The continuous increase in the number of coarse crystals indicates growth into the range $>250\ \mu$m, rather than nucleation events. This result, which is in accordance to the mechanism of Ostwald ripening, shows that DNC is able to provide *in situ* automatic fine removal without the need for additional equipment or design. The DNC experiments at 3000 and 4000 #/s also produced similar results and trends. Figures 7(a) and (b) show the profiles of number of counts/s with the addition of antisolvent/solvent and the evolution of fine and coarse crystals, respectively, during the DNC experiment at 3000 #/s. As before, after a couple of overshoots and undershoots before the system finally reached the desired number of counts/s.

Figure 8 shows the profile of number of counts/s for all the controlled experiments. It was found that the smallest desired number of counts/s was more difficult to control, and it gave higher noise due to the smaller particle concentration. The results show that different set-points consistently produced similar solvent/antisolvent addition output profiles. This suggests that an iterative learning control approach[35] could be used to eliminate the over- and undershoots during the first part of the batch and to enhance the overall control performance of the DNC. According to this approach, a feedforward plus feedback controller could be implemented, in which the feedforward law given by the solvent/antisolvent addition profile would be iteratively improved in a batch-to-batch manner so that the overall control error would decrease throughout consecutive batches. The feedforward component of the iterative learning control would provide batch-to-batch performance improvement, whereas the feedback control component would minimize the effects of within batch disturbances. The iterative learning control approach would improve performance and would provide increased robustness for industrial implementation. However, the benefits of DNC in producing higher quality crystals at the end of the batch are evident already from the implementation demonstrated in this paper, as discussed below.

Figure 9 compares the plots of SWMCLs for the uncontrolled and DNC experiments at 2000 and 4000 #/s. The plot of SWMCL for the DNC experiment at 3000 #/s is omitted to prevent overcrowding, but it was found to stabilize between

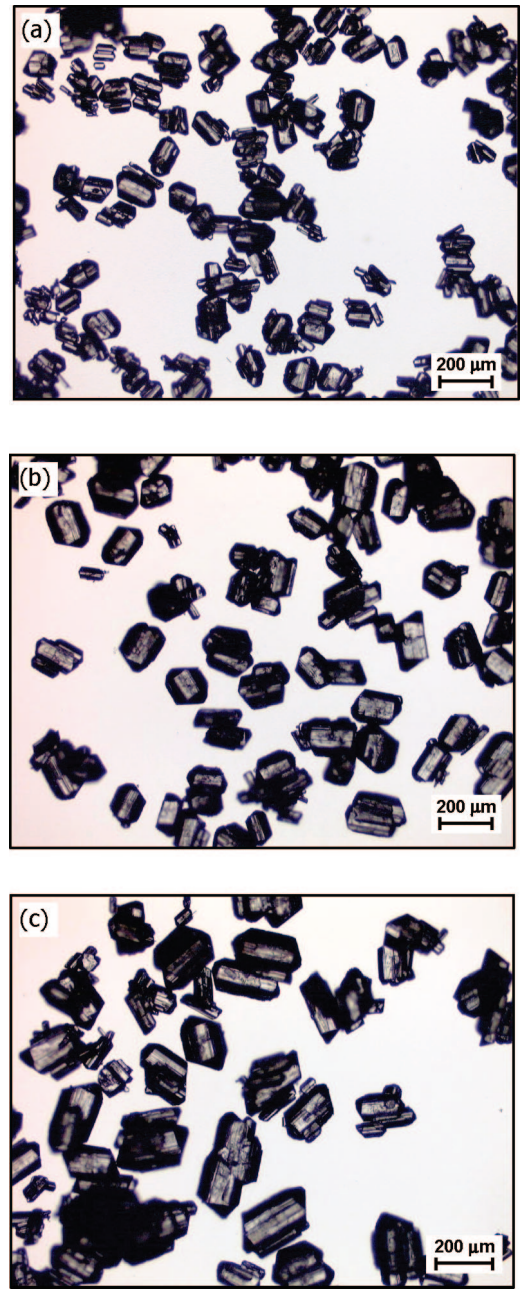


**Figure 10.** Microscopic images of crystals obtained from (a) uncontrolled, (b) DNC at 4000 #/s, and (c) DNC at 2000 #/s experiments.

those of 2000 and 4000 #/s. Based on Figure 9, the growth of the crystals was a maximum in the experiment with the lowest counts/s set-point, and a minimum in the uncontrolled experiment. The calculated values of the SWMCL for the controlled number of counts/s at 2000 #/s, 3000 #/s, 4000 #/s and uncontrolled experiments are 281, 268, 263 and 232 $\mu$m respectively. The SWMCL values shown in Figure 9 are more scattered since the smaller the number of particles in the system, the higher the noise in the statistics of the CSD, leading to an increased difficulty in controlling the system at lower counts/s set-points. This is exemplified by the controlled experiment at 2000 #/s, which has the most scattered SWMCL values. The smaller the number of particles, the larger the crystals will grow, however the corresponding increased noise in the measurement requires a suitable compromise when selecting the set-point counts/s values for the DNC.

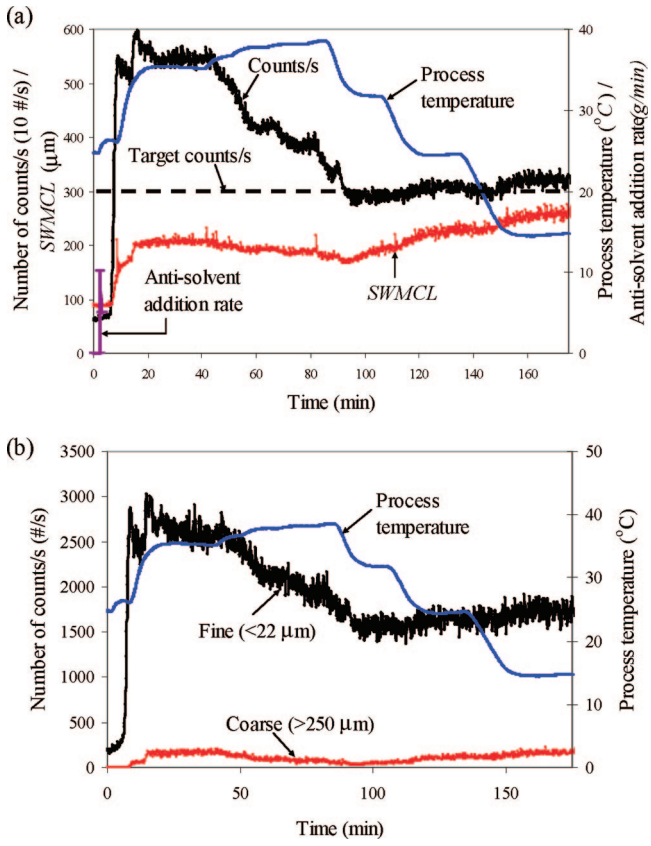


**Figure 11.** Profiles of (a) number of counts/s, SWMCL, process temperature, and antisolvent addition rate, and (b) number of fine and coarse particles, and process temperature in the DNC experiment by a combined approach.

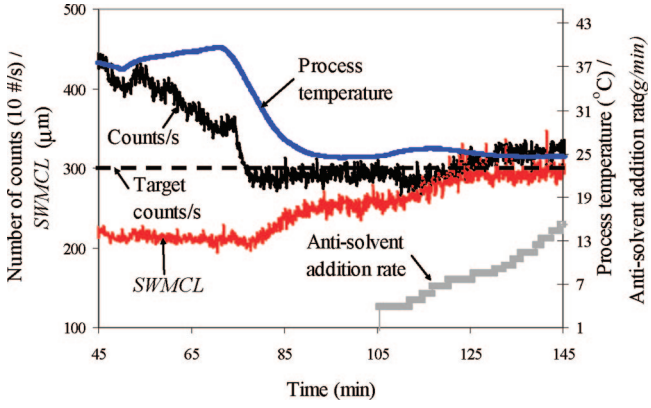


**Figure 12.** Profiles of number of counts/s, SWMCL, process temperature, and antisolvent addition rate in the DNC by an alternative combined approach.

Figure 10 shows the microscopic images of the crystals at the end of the experiments, which confirmed the results obtained from FBRM. Based on the images, the size of crystals obtained from the controlled experiment at the lower counts/s, i.e. 2000 #/s, was generally found to be the largest, while the size of crystals obtained from the uncontrolled experiments was found to be the smallest.

The DNC by antisolvent/solvent addition requires a large volume crystallizer since it involves addition of antisolvent and solvent. This limitation of the approach may be critical as it requires additional cost for a large volume vessel. Furthermore, the large volume of suspension which results from the addition of antisolvent and solvent may lead to mixing problems. Another problem is the generation of large volumes of waste materials that are costly to separate.

**4.4. DNC by Combined Antisolvent Addition and Heating−Cooling.** In these experiments the hard constraint of limited vessel capacity was relaxed by using heating/cooling to control the level of supersaturation instead of solvent/antisolvent additions. In this approach, the vessel's volume requirement is only to accommodate the initial antisolvent addition for generating the nuclei.

Figure 11(a) shows the profiles of number of counts/s, SWMCL, process temperature, and antisolvent addition rate for the experiment using the combined approach of antisolvent addition and heating−cooling, with a target number of counts/s of 3000 #/s. Initially, when the number of counts/s went beyond the desired value upon nucleation as a result of the antisolvent addition, the addition was stopped and, subsequently, the temperature was increased gradually, depending on the error between the measured and desired number of counts/s, to dissolve the excessive nuclei. The number of counts/s gradually decreased as the temperature was increased. As soon as the number of counts/s went below 4000 #/s, cooling was initiated. The number of counts/s eventually settled at 3000 #/s. They remained approximately at the same level throughout the process, even when the system was cooled down to 15 °C at the maximum rate, set to 0.3 °C/min. This continuous cooling was required to generate the supersaturation for crystal growth.

The profile of SWMCL of the system during the experiment shows that the mean size of the crystals was not affected very much by the heating, only reduced slightly at high temperature (approximately at 38 °C). As confirmed by the trends of the evolution of fines and coarse crystals during DNC in Figure 11(b), the heating dissolves only fine crystals, which do not contribute a lot to the SWMCL. As the cooling continues, the mean size of the crystals increased significantly as shown by the steady increase of the SWMCL (Figure 11(a)). It can also be seen that, during cooling, there was a slight increase in the number of counts/s due to secondary nucleation. However, during the second part of the batch the process is dominated by growth and the amount of fines generated was not significant enough to trigger the dissolution mechanism of the DNC. In this experiment, the amount of ethanol consumed was very little (53 g), as it was only used to initiate the nucleation.

As an alternative to cooling toward the end of the batch for supersaturation generation, hence promoting growth, the application of antisolvent addition was also tested. Figure 12 shows the profiles of the number of counts/s, SWMCL, process temperature and antisolvent addition rate during the last 100 min of the experiment.

The figure shows that the crystals started to grow in size with cooling and then further growth was promoted with the addition of antisolvent. Although antisolvent was continuously added, the growth rate decreased significantly after about 125 min. The solubility of glycine has a lower sensitivity to the solvent/antisolvent ratio as the amount of antisolvent increases in the system (see Figure 4). The decrease in the growth is probably due to the fact that, as the sensitivity in the solubility decreases, the dilution effect becomes predominant in decreasing the supersaturation, thus depleting the driving force for growth (see Figure 4).

In comparison, the calculated SWMCL for the crystals obtained from antisolvent addition toward the end is 297 $\mu$m, whereas that obtained from cooling alone toward the end is 258 $\mu$m. However, the former consumed a significantly larger amount of ethanol (730 g). The batch time of DNC by the

**Table 1. Different DNC Strategies To Reach a Stabilized Desired Counts/s of 3000 and Their Resultant Batch Times, Amount of Antisolvent Used and SWMCL of the Crystals Obtained**

| DNC strategy | batch time (min) | amount of antisolvent used (g) | SWMCL of crystals obtained ($\mu$m) |
|---|---|---|---|
| addition of antisolvent to nucleate; control of counts/s by additions of solvent and antisolvent; antisolvent addition toward the end to promote growth | 68 | 370 | 268 |
| addition of antisolvent to nucleate; control of counts/s by heating and cooling; cooling toward the end to promote growth | 168 | 53 | 258 |
| addition of antisolvent to nucleate; control of counts/s by heating and cooling; antisolvent addition toward the end to promote growth | 145 | 730 | 297 |

combined approach was longer than that of DNC by antisolvent/solvent addition because heating/cooling gave a slower response. Table 1 compares the outcomes of applying different DNC strategies to reach a stabilized desired counts/s of 3000.

Suitable automatic control of the solvent/antisolvent addition or heating and cooling is difficult especially during the initial part of the batch when the first nucleation events are generated. The initial overshoot can be minimized by automatically stopping the antisolvent addition when a continuous increase in the number of counts/s has been detected, but before the desired set-point is achieved. The overshoots can be minimized by using a control structure with antiwindup which allows an immediate switch from antisolvent addition to solvent addition (or from cooling to heating), and vice versa when the desired set-point is achieved. An iterative learning control approach could lead to batch-to-batch improvement in the performance of the DNC. Although in the case of the model system used in this work (glycine in water) attrition or agglomeration was not observed, these are common phenomena in the case of industrial crystallization systems, and are not accounted for either by the supersaturation control or by the classical open-loop control approaches. The DNC approach could have the additional benefits in the control of systems exhibiting these phenomena. The fines generated by attrition would be detected as an increase in the number of counts/s and hence would be eliminated by the DNC, by controlled dissolution. Additionally, the particular feature of the DNC approach of generating partial dissolution by repeatedly driving the process into the undersaturated regime has a beneficial deagglomeration effect.

## 5. Conclusions

The direct nucleation control (DNC) approach implemented in this work controls directly the amount of nuclei present using information provided by FBRM, in a feedback control strategy through (i) addition of antisolvent or reduction of the suspension temperature to generate nuclei up to a desired number of counts/s and (ii) addition of solvent or increment of the suspension temperature to correct the nuclei count, should excess nucleation occur. It has been found that the DNC approach implemented in these experiments, using glycine in water−ethanol mixture as a model system, was able to produce crystals with a larger size than those obtained from uncontrolled experiments. Results also suggest that the lower the desired number of counts/s, the larger the size of the crystals produced. In the experiments which used the application of the combined approach, the results indicate that the crystals produced were even larger. In some cases better control of nuclei generation and correction are still needed, but nonetheless the approach has proved to provide a robust crystallization control strategy.

**Acknowledgment.** Financial support provided by the Engineering and Physical Sciences Research Council (EPSRC), U.K. (Grant EP/E022294/1), is gratefully acknowledged. One of the authors (M.R.A.B.) is grateful to the Malaysian Ministry of Higher Education and the International Islamic University Malaysia for a scholarship.

## References

(1) Reutzel-Edens, S. M. *Curr. Opin. Drug Discovery Dev.* **2006**, *9*, 806–815.
(2) Yu, L. X.; Lionbergera, R. A.; Rawa, A. S.; D'Costa, R.; Wub, H.; Hussain, A. S. *Adv. Drug Delivery Rev.* **2004**, *56*, 349–369.
(3) Barrett, P.; Smith, B.; Worlitschek, J.; Bracken, V.; O'Sullivan, B.; O'Grady, D. *Org. Process Res. Dev.* **2005**, *9*, 348–355.
(4) Birch, M.; Fussell, S. J.; Higginson, P. D.; McDowall, N.; Marziano, I. *Org. Process Res. Dev.* **2005**, *9*, 360–364.
(5) Braatz, R. D. *Annu. Rev. Control* **2002**, *26*, 87–99.
(6) Larsen, P. A.; Patience, D. B.; Rawlings, J. B. *IEEE Control Syst. Mag.* **2006**, *26*, 70–80.
(7) Worlitschek, J.; Mazzotti, M. *Cryst. Growth Des.* **2004**, *4*, 891–903.
(8) Gron, H.; Borissova, A.; Roberts, K. J. *Ind. Eng. Chem. Res.* **2003**, *42*, 198–206.
(9) Nonoyama, N.; Hanaki, K.; Yabuki, Y. *Org. Process Res. Dev.* **2006**, *10*, 727–732.
(10) Yu, Z. Q.; Chow, P. S.; Tan, R. B. H. *Ind. Eng. Chem. Res.* **2006**, *45*, 438–444.
(11) Fujiwara, M.; Nagy, Z. K.; Chew, J. W.; Braatz, R. D. *J. Process Control* **2005**, *15*, 493–504.
(12) Zhou, G. X.; Fujiwara, M.; Woo, X. Y.; Rusli, E.; Tung, H.; Starbuck, C.; Davidson, O.; Ge, Z.; Braatz, R. D. *Cryst. Growth Des.* **2006**, *6*, 892–898.
(13) Nagy, Z. K.; Chew, J. W.; Fujiwara, M.; Braatz, R. D. *J. Process Control* **2008**, *18*, 399–407.
(14) Ward, J. D.; Mellichamp, D. A.; Doherty, M. F. *AIChE J.* **2006**, *52*, 2046–2054.
(15) Barrett, P.; Glennon, B. *Chem. Eng. Res. Des.* **2002**, *80*, 799–805.
(16) Barthe, S.; Rousseau, R. W. *Chem. Eng. Technol.* **2006**, *29*, 206–211.
(17) Chew, J. W.; Black, S. N.; Chow, P. S.; Tan, R. B. H. *Ind. Eng. Chem. Res.* **2007**, *46*, 830–838.
(18) Chew, J. W.; Chow, P. S.; Tan, R. B. H. *Cryst. Growth Des.* **2007**, *7*, 1416–1422.
(19) Liotta, V.; Sabesan, V. *Org. Process Res. Dev.* **2004**, *8*, 488–494.
(20) Fujiwara, M.; Chow, P. S.; Ma, D. L.; Braatz, R. D. *Cryst.l Growth Des.* **2002**, *2*, 363–370.
(21) Nagy, Z. K.; Fujiwara, M.; Woo, X. Y.; Braatz, R. D. *Ind. Eng. Chem. Res.* **2008**, *47*, 1245–1252.
(22) Doki, N.; Seki, H.; Takano, K.; Asatani, H.; Yokota, M.; Kubota, N. *Cryst. Growth Des.* **2006**, *4*, 949–953.
(23) Tadayyon, A.; Rohani, S. *Can. J. Chem. Eng.* **2000**, *78*, 663–673.
(24) Sheikhzadeh, M.; Trifkovic, M.; Rohani, S. *Chem. Eng. Sci.* **2008**, *63*, 991–1002.
(25) Sheikhzadeh, M.; Trifkovic, M.; Rohani, S. *Chem. Eng. Sci.* **2008**, *63*, 1261–1272.
(26) Woo, X. Y.; Nagy, Z. K.; Tan, R. B. H.; Braatz, R. D. *Cryst. Growth Des.* **2009**, in press.
(27) Lewiner, F.; Fevotte, G.; Klein, J. P.; Puel, F. *Ind. Eng. Chem. Res.* **2002**, *41*, 1321–1328.
(28) Nagy, Z. K.; Braatz, R. D. *AIChE J.* **2003**, *49* (7), 1776–1786.
(29) Hermanto, M. W.; Chiu, M.-S.; Woo, X. Y.; Braatz, R. D. *AIChE J.* **2007**, *53*, 2643–2650.
(30) Mullin, J. W. *Crystallization*; Butterworth-Heinemann: London, 2001.
(31) Nozaki, Y.; Tanford, C. *J. Biol. Chem.* **1971**, *246*, 2211–2217.
(32) Dunn, M. S.; Ross, F. J. *J. Biol. Chem.* **1937**, *125*, 309–332.
(33) Heath, A. R.; Fawell, P. D.; Bahri, P. A.; Swift, J. D. *Part. Part. Syst. Charact.* **2002**, *19*, 84–95.
(34) Yu, W.; Erickson, K. *Powder Technol.* **2008**, *185*, 24–30.
(35) Lee, K. S.; Lee, J. H. *J. Process Control* **2003**, *13*, 607–621.

CG800595V